

LUMINOUS COMPACT BLUE GALAXIES IN INTERMEDIATE-REDSHIFT GALAXY CLUSTERS: A SIGNIFICANT BUT EXTREME BUTCHER-OEMLER POPULATION

S. M. CRAWFORD, M. A. BERSHADY, A. D. GLENN, AND J. G. HOESSEL

Washburn Observatory, University of Wisconsin–Madison, 475 North Charter Street, Madison, WI 53706; crawford@astro.wisc.edu

Received 2005 September 13; accepted 2005 November 16; published 2005 December 12

ABSTRACT

We identify a population of luminous compact blue galaxies (LCBGs) in two galaxy clusters: MS 0451.6–0305 ($z = 0.54$) and Cl 1604+4304 ($z = 0.9$). LCBGs are identified via photometric characteristics and photometric redshifts derived from broad- and narrowband images taken with the WIYN telescope and the *Hubble Space Telescope* (*HST*). We analyze their surface densities and clustering properties to find that they compose a statistically significant portion (42% and 53%, respectively) of the Butcher-Oemler (BO) galaxies in both clusters and that their spatial distributions are best characterized by a shell model. The enhancement of the projected space density of LCBGs with $M_B < -18.5$ in the clusters relative to the field is 3–10 times higher than the BO population as a whole but 2 times lower than the red population, except in the core where LCBGs are absent. Assuming some fading, a natural descendant would be small, low-luminosity galaxies found preferentially in today’s clusters, such as dE galaxies.

Subject headings: galaxies: clusters: general — galaxies: clusters: individual (Cl 1604+4304, MS 0451.6–0305) — galaxies: evolution — galaxies: photometry — galaxies: starburst

1. INTRODUCTION

The number of blue, star-forming galaxies increases in all environments at intermediate redshifts ($0.3 < z < 1.0$). In the field, there is a dramatic rise in the space density of luminous¹ ($M_B \sim -20$), compact ($R_e \sim 2$ kpc), and blue ($B - V \sim 0.35$) galaxies known as LCBGs (Koo et al. 1994; Guzmán et al. 1997). These galaxies produce stars at such a tremendous rate ($1\text{--}40 M_\odot \text{ yr}^{-1}$; Hammer et al. 2001) that they provide a substantial fraction of the star formation in the universe at $0.4 < z < 1$ (Guzmán et al. 1997). In clusters, Butcher & Oemler (1978, 1984) claimed that the fraction of blue galaxies increases with redshift. Blue cluster galaxies have been classified as a mix of normal galaxies absent in local clusters, morphologically disturbed, and star-forming galaxies (Oemler et al. 1997). Recent studies indicate that star-forming galaxies in intermediate-redshift clusters are typically small, disklike (de Propris et al. 2003; Lotz et al. 2003; Finn et al. 2004), and falling into the cluster (Balogh et al. 2000; Homeier et al. 2005; Tran et al. 2005) in groups and clumps (Kodama et al. 2001). While several studies exist for LCBGs in the field and Koo et al. (1997) have identified a handful of LCBGs in Cl 0024, no thorough census of LCBGs in clusters has been completed.

Field LCBGs and cluster star-forming galaxies have been proposed as the progenitors of dwarf elliptical (dE) galaxies (Koo et al. 1994; Guzmán et al. 1997; Koo et al. 1997; Martin et al. 2000) or low-mass S0 galaxies (Tran et al. 2005). The line widths and physical sizes of field and cluster LCBGs are consistent with those of dwarf elliptical galaxies (or field “dE’s” like NGC 205). Recent bursts inferred from the stellar histories of local dwarf ellipticals (Grebel et al. 2003) and in nearby clusters (Poggianti et al. 2001; Conselice et al. 2001) support a fading scenario. LCBGs are viable candidates to explain, and eventually fill in, the missing faint red sequence of galaxies seen at $z \sim 0.75$ (de Lucia et al. 2004; Goto et al. 2005). However, the high masses (Phillips et al. 1997, hereafter P97), high metallicities (Kobulnicky & Zaritsky 1999), large extinctions

(Hammer et al. 2001), and centrally concentrated starbursts (Barton & van Zee 2001) seen in some LCBGs make them plausible candidates to be a burst phase of more massive spiral galaxies. Both dE’s and more massive bulges are accreted populations in local clusters (Conselice et al. 2001; Biviano et al. 2002), but they have very different morphology-density relationships (Ferguson & Binggeli 1994). Understanding the prevalence and distribution of LCBGs in clusters should constrain their role as a progenitor population.

In this Letter we measure the density and clustering properties of LCBGs in two rich clusters (Table 1): MS 0451.6–0305 and Cl 1604+4304. MS 0451 is an incredibly rich, X-ray-bright cluster (Ellingson et al. 1998; Donahue et al. 2003). Cl 1604+4304 is part of a supercluster complex (Postman et al. 2001; Lubin et al. 2004; Gal & Lubin 2004) but is not as X-ray-luminous. The cluster redshifts span an epoch where the dynamical mass of field LCBGs changes rapidly (P97), and they are sufficiently disparate to permit the derivation of complementary field samples using the same data.

2. OBSERVATIONS AND ANALYSIS

Observations were obtained with the WIYN² 3.5 m telescope’s Mini-Mosaic Camera ($0''.14 \text{ pixel}^{-1}$ and $9'.6 \times 9'.6$ field of view) and augmented with archival *HST* WFPC2 and ACS images for both clusters, reduced via the standard *HST* reduction pipeline. MS 0451 is sampled by images in the F775W, F814W, and F850LP bandpasses; Cl 1604 is imaged in F606W and F814W. Harris *UBRI*, Gunn z , and two narrowband filters³ were obtained at WIYN between 1999 October and 2004 June. We use data from nights with good transparency and seeing (FWHM $\sim 0.85^{+0.45}_{-0.35}$ arcsec).

Reduced Mini-Mo images are flat to within 1% of their initial

² The WIYN Observatory is a joint facility of the University of Wisconsin–Madison, Indiana University, Yale University, and the National Optical Astronomy Observatories.

³ On-band filters were custom-made narrowband ($\lambda/\Delta\lambda \sim 70$) filters sampling rest-frame [O II] $\lambda 3727$. Off-band filters were NOAO filter KP1582 ($\lambda/\Delta\lambda \sim 20$) for MS 0451 and another custom filter ($\lambda/\Delta\lambda \sim 70$) for Cl 1604.

¹ We adopt $H_0 = 70 \text{ km s}^{-1} \text{ Mpc}^{-1}$, $\Omega_M = 0.3$, and $\Omega_\Lambda = 0.7$.

TABLE 1
CLUSTER PROPERTIES

Cluster	R.A. (J2000)	Decl. (J2000)	z	σ (km s ⁻¹)	L_x^a (ergs s ⁻¹)	R_c (Mpc)	R_{200}^b (Mpc)
MS 0451	04 54 10.8	-03 00 56	0.538	1354	1.4×10^{45}	0.18	1.64
Cl 1604	16 04 18.2	+43 04 38	0.90	982	8.6×10^{43}	0.14	1.48

NOTE.—Units of right ascension are hours, minutes, and seconds, and units of declination are degrees, arcminutes, and arcseconds.

^a L_x is measured in the 0.3–3.5 and 0.5–2.0 keV bands, respectively, for MS 0451 and Cl 1604.

^b R_{200} is the radius where the cluster density is 200 times the critical density (Finn et al. 2004).

sky values. We created deep mosaics by combining only high-quality data weighted by the ratio of the flux from an average star to the square root of the sky deviation and seeing for that image (Bershady et al. 1998). Data were calibrated through (1) spectrophotometric standard stars (Massey et al. 1988) and Landolt (1992) photometric stars observed during the WIYN 3.5 m runs; (2) observations of Landolt (1992) standards and cluster fields at the WIYN 0.9 m telescope; (3) comparisons to the *HST* WFPC2 and ACS observations; and (4) comparison of the observed stellar locus to that derived for our filter set from the Gunn-Stryker catalog (Gunn & Stryker 1983). Through these methods, we estimate that relative and absolute calibration uncertainties are below 2%, assuming that no large metallicity differences exist between the Gunn-Stryker catalog and our field stars.

Object detection was performed on the sum of the *UBRIZ* images using SExtractor (Bertin & Arnouts 1996) with the criterion that objects contained >20 contiguous pixels above 3σ of the sky noise. Detection completeness was determined via Monte Carlo simulations reinserting real objects back into the images. Total magnitudes and half-light radii are determined from light-profile curves of growth. Total magnitudes are set to the flux within an aperture that is a multiple of the $\eta = 0.2$ radius (η is the Petrosian ratio as defined by Kron 1995). The multiplier is determined from the light-concentration parameter, C_{2080} (Bershady et al. 2000). With this “tailored” aperture, total magnitudes are measured to within an accuracy of 1% regardless of profile shape (e.g., only 80% of the light is enclosed where $\eta = 0.2$ for an $r^{1/4}$ profile; Graham et al. 2005). Colors were determined within a seeing-matched aperture of radius $1.5 \times \text{FWHM}$ in each image. Photometric precision is

0.1 mag at $R = 24.25$ and 25 for total and seeing-matched apertures, respectively. Random errors for total magnitudes depend on the light-profile shape; $r^{1/4}$ -law profile errors are larger than the values quoted here for exponential profiles.

Photometric redshifts are determined through a method similar to that of Csabai et al. (2003). We convolved a standard set of model and observed galaxy templates with our filters to produce a template-redshift grid for $0 < z < 5$ and $\Delta z = 0.01$. Both fields have close to 100 galaxies with spectroscopic redshifts (Ellingson et al. 1998; Postman et al. 2001). For each field we match galaxies with high-quality spectroscopic redshifts and good photometry with points on the template-redshift grid, and correct the grid for differences between the simulated and measured colors. The trained grids yield photometric redshifts for every object with a precision $\sigma_z < 0.05$ (blue objects) and 0.03 (red objects) to $z = 1.0$ and $S/N > 10$.

Absolute magnitudes, radii, rest-frame surface brightness, and colors were calculated for all objects using photometric or spectroscopic redshifts. *K*-correction calculations adopt method 4 of Bershady (1995). Half-light radii were measured in the band closest to rest-frame *B* and corrected for point-spread function effects by quadrature subtraction of the stellar half-light radius. Surface brightnesses in the WIYN images were corrected for seeing using measurements from the overlapping regions with the *HST* data. WIYN-based surface brightnesses have a 1.5 mag dispersion due to seeing-correction effects on the measured radii.

3. IDENTIFICATION OF LCBGS

We define LCBGS here as “enthusiastic” star-forming galaxies. For these purposes, we define LCBGS as having the following properties: $(B - V)_0 < 0.5$ and $\bar{\mu}_e(B) < 21$ mag arcsec⁻², where $\bar{\mu}_e$ is the rest-frame *B*-band average surface brightness within the half-light radius. A galaxy with $L_{\text{bol}} = 10^9 L_\odot$ and a constant star formation rate will have $(B - V)_0 < 0.4$ and $\bar{\mu}_e(B) < 20.5$ for ages more than a few $\times 10^8$ yr. A moderate amount of extinction, e.g., $E(B - V) = 0.1$, will leave the galaxy with the above parameters. Anything bluer or brighter will be more than an enthusiastic star former. The selection region for LCBGS is plotted in Figure 1. This region is mostly devoid of objects in local surveys (e.g., Werk et al. 2004; Garland et al. 2004) and is purposely constructed to identify actively star-forming galaxies that are extreme compared to the local universe in clusters or the field. For comparison with other LCBG samples and to differentiate them from “dwarf” galaxies (at least in luminosity), we also require LCBGS to have $M_B < -18.5$.

Galaxies were selected from the ground-based data set. We estimate that, based on extant *HST* data, this selection misses ~5% of the bona fide LCBGS (primarily due to the error in the size measurement), while introducing the same percentage of false classifications. We identified “cluster” galaxies in our sample—including LCBGS—as having a photometric redshift within

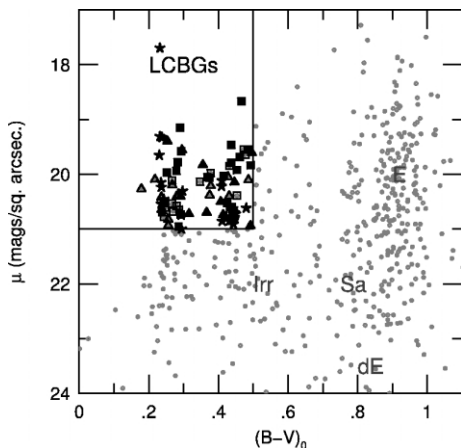


FIG. 1.—Rest-frame surface brightness vs. color for cluster LCBGs (filled symbols) and field LCBGs (open symbols) found in the *HST* images of MS 0451 and Cl 1604, and for field LCBGs from P97 (stars). Other intermediate-redshift galaxies in our fields are shown as gray points. Lines mark the selection criteria for LCBGS used here. Labels indicate $z = 0$ galaxy types.

± 0.1 of the cluster’s redshift and a reasonable probability to be at the cluster redshift based on the individual photometric error and measurements from the training set (Brunner & Lubin 2000). Within 1 Mpc of the clusters’ centers, we find 41 candidate LCBGs. Four objects are confirmed as cluster members through spectroscopic redshifts, and 23 are confirmed by having strong emission (equivalent width greater than 10 \AA) in the “on” narrowband image, which samples rest-frame $[\text{O II}] \lambda 3727$. We have three objects that are identified as cluster LCBGs but that have spectroscopic redshifts, placing them outside of the cluster (still within a redshift of 0.1 of the cluster), and weak $[\text{O II}]$ emission. The remaining 10 objects require spectroscopic follow-up to confirm cluster membership.

We select two other groups of luminous ($M_B < -18.5$) cluster galaxies in our data, red and blue, to compare to the LCBG population. We fit the color-magnitude relationship in both clusters, splitting the population according to the classic definition of the Butcher-Oemler effect (Butcher & Oemler 1978, 1984): $|\Delta(B - V)_0| > 0.2$ are “BO” galaxies, which include the LCBG population. The remainder are the red cluster sequence. We measure $f_b = 0.22 \pm 0.05$ within $R = 0.5$ Mpc, rising to 0.33 ± 0.04 at $R = 1.5$ Mpc in MS 0451, in good agreement with Ellingson et al. (2001) and de Propris et al. (2003). For CI 1604, we measure $f_b = 0.5 \pm 0.13$ within $R = 0.5$ Mpc, rising to 0.63 ± 0.07 at $R = 1.5$ Mpc, as compared to the values of $f_b = 0.8$ as measured by Rakos & Schombert (1995).

4. THE NUMBER DENSITY AND DISTRIBUTION OF CLUSTER LCBGs

We plot the surface density of galaxies in Figure 2 as a function of radius from the cluster center (defined as the brightest cluster galaxy). The data extend to a radius where our completeness is still uniform in the WIYN images. Two basic results emerge. (1) All populations clearly show evidence of clustering. (2) LCBGs form a statistically significant population in both clusters: $14\% \pm 4\%$ and $34\% \pm 9\%$ of the total population at R_{200} and $M_B < -18.5$ (for MS 0451 and CI 1604, respectively), and $42\% \pm 11\%$ and $53\% \pm 14\%$ of the BO galaxies in each cluster. (Errors are likely non-Gaussian and arise from cluster-membership uncertainties.) For comparison, we estimate that LCBGs constitute approximately 8% and 26% of all field galaxies blue enough to be classified as “BO” at $z = 0.5$ and 0.9, respectively.

We model the projected distribution of the LCBG, BO, and red cluster populations with a King profile (King 1972) and two spherical-shell density profiles. The King radius is set to the scale radius of the X-ray profile for each cluster (Donahue et al. 2003; Lubin et al. 2004). Spherical-shell models are empty inside of the X-ray scale radius (“shell”) or half this value (“half-shell”), and then both decline as a King profile with a 1 Mpc core radius. The King model fits all of the populations well in a χ^2 sense. The red population is only fit well by the King model; the BO populations are best fit by the half-shell model; and LCBGs in MS 0451 are best fit by the shell model, whereas the CI 1604 LCBGs are best fit by the half-shell model. If LCBGs are distributed as a King profile, there is a 95% probability that we would detect ≥ 1 LCBG in the inner 0.15 Mpc region of MS 0451. Therefore, LCBGs do not appear to exist in central cluster regions—in agreement with the Homeier et al. (2005) findings for star-forming galaxies in CI 0152 ($z = 0.84$).

We compare the surface density of cluster objects to the same objects in the field. Red and BO galaxy field densities are calculated from the luminosity function of the DEEP2 data

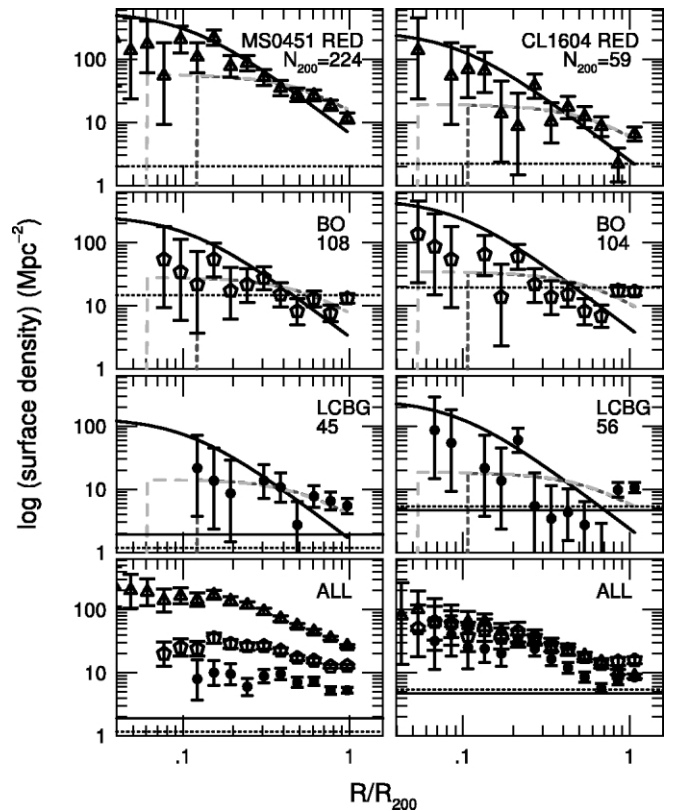


Fig. 2.—Surface densities for cluster galaxies. The top six panels are the differential distributions of red galaxies (triangles), BO galaxies (pentagons), and LCBGs (circles) for MS 0451 and CI 1604. Model curves (see text) are for a King profile (solid curve) and shell models (dashed line) based on the X-ray light profile. Dotted lines represent field densities for each class at the cluster redshift (see text). Solid lines are the LCBG field density as measured in our “off” image. The number, N_{200} , is the number of objects at R_{200} in each respective class. The two bottom panels show mean surface densities.

(Faber et al. 2005). With our selection criteria, the field LCBG surface density derived from the P97 sample yields 1.2 and 5.44 Mpc^{-2} at $z = 0.53$ and $z = 0.90$, respectively, after applying corrections due to their selection effects. We also use foreground LCBGs in the CI 1604 field to estimate the field density of LCBGs at $z \sim 0.5$, and vice versa for MS 0451, to find 1.9 ± 0.8 and $4.7 \pm 1.2 \text{ Mpc}^{-2}$ at $z = 0.53$ and $z = 0.90$ for objects with $M_B < -18.5$. Field densities are calculated in the same redshift bin size and manner as the cluster samples. We couch our comparison between the two objects in terms of “enhancement”: the surface density ratio of cluster to field. The enhancement as a function of cluster-galaxy surface density (Fig. 3) shows that red galaxies behave qualitatively as expected according to the morphology-density relationship (Dressler et al. 1997). The BO galaxies show only a modest enhancement and trend with surface density. LCBGs display a larger enhancement, increasing with luminous ($M_B < -18.5$) galaxy surface density but dropping precipitously at surface densities above 150 Mpc^{-2} .

5. DISCUSSION

We find that LCBGs in two intermediate-redshift clusters compose a significant fraction of the BO populations despite the clusters’ different redshifts, environments (X-ray luminosities and projected densities), and relative blue fractions. At lower redshift and greater “richness” (MS 0451), there is clear segregation in the surface densities of subpopulations with red :

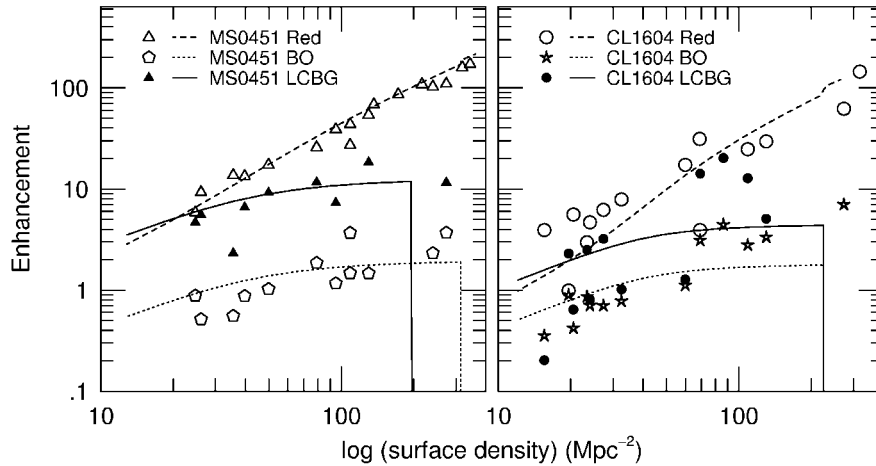


FIG. 3.—Cluster galaxy enhancement relative to the field as a function of cluster surface density (for galaxies with $M_B < -18.5$ within circular annuli about the cluster center). The lines are the best-fit models to each population.

BO : LCBG = 26.6 : 12.9 : 5.4 Mpc^{-2} within R_{200} . In CL 1604 the different populations have comparable densities (red : BO : LCBG = 8.9 : 15.8 : 8.5 Mpc^{-2}). At luminous galaxy surface densities of 100 Mpc^{-2} , the enhancement of these different subpopulations relative to the field are a factor of 2–4 for BO galaxies, 8–20 for LCBGs, and 30–50 for red galaxies in both clusters. This is suggestive of LCBGs as progenitors of populations found preferentially in clusters today. Because LCBGs show significant enhancement variations between clusters and with surface density, a secure interpretation of LCBGs as a progenitor population awaits better sampling of environment and redshift. An analysis of 10 clusters in the range $0.3 < z < 1.0$ is forthcoming. Here we suggest that since they appear to be physically small, if LCBGs fade, dE and low-mass S0 galaxies would be one plausible remnant population.

Despite their similar spatial distribution, LCBGs are an extreme subcomponent of the BO population in terms of their

cluster enhancement, color, and surface brightness. If LCBGs are on predominantly radial orbits, their cluster-shell enhancement indicates initial infall—a spectroscopically testable claim. In this scenario, their starbursts are plausibly triggered through galaxy interactions in the cluster periphery, where densities are enhanced but where interaction times are still long, or via interactions with the intercluster medium (ICM). The former supposition is testable via angular correlation measurements of large samples. A correlation between the X-ray emission and position of the LCBGs would support an ICM-driven trigger for the starbursts.

We thank the anonymous referee for helpful comments. Research was supported by STScI/AR-9917, NSF/AST-0307417, and a Wisconsin Space Grant. Some of the data presented in this Letter were obtained from STScI/MAST.

REFERENCES

- Balogh, M. L., Navarro, J. F., & Morris, S. L. 2000, *ApJ*, 540, 113
 Barton, E. J., & van Zee, L. 2001, *ApJ*, 550, L35
 Bershad, M. A. 1995, *AJ*, 109, 87
 Bershad, M. A., Jangren, A., & Conselice, C. J. 2000, *AJ*, 119, 2645
 Bershad, M. A., Lowenthal, J. D., & Koo, D. C. 1998, *ApJ*, 505, 50
 Bertin, E., & Arnouts, S. 1996, *A&AS*, 117, 393
 Biviano, A., Katgert, P., Thomas, T., & Adami, C. 2002, *A&A*, 387, 8
 Brunner, R. J., & Lubin, L. M. 2000, *AJ*, 120, 2851
 Butcher, H., & Oemler, A. 1978, *ApJ*, 226, 559
 ———. 1984, *ApJ*, 285, 426
 Conselice, C. J., Gallagher, J. S., & Wyse, R. F. G. 2001, *ApJ*, 559, 791
 Csabai, I., et al. 2003, *AJ*, 125, 580
 de Lucia, G., et al. 2004, *ApJ*, 610, L77
 de Propris, R., Stanford, S. A., Eisenhardt, P. R., & Dickinson, M. 2003, *ApJ*, 598, 20
 Donahue, M., Gaskin, J. A., Patel, S. K., Joy, M., Clowe, D., & Hughes, J. P. 2003, *ApJ*, 598, 190
 Dressler, A., et al. 1997, *ApJ*, 490, 577
 Ellingson, E., Lin, H., Yee, H. K. C., & Carlberg, R. G. 2001, *ApJ*, 547, 609
 Ellingson, E., Yee, H. K. C., Abraham, R. G., Morris, S. L., & Carlberg, R. G. 1998, *ApJS*, 116, 247
 Faber, S. M., et al. 2005, *ApJ*, submitted (astro-ph/0506044)
 Ferguson, H. C., & Bingeli, B. 1994, *A&A Rev.*, 6, 67
 Finn, R. A., Zaritsky, D., & McCarthy, D. W. 2004, *ApJ*, 604, 141
 Gal, R. R., & Lubin, L. M. 2004, *ApJ*, 607, L1
 Garland, C. A., Pisano, D. J., Williams, J. P., Guzmán, R., & Castander, F. J. 2004, *ApJ*, 615, 689
 Goto, T., et al. 2005, *ApJ*, 621, 188
 Graham, A. W., Driver, S. P., Petrosian, V., Conselice, C. J., Bershad, M. A., Crawford, S. M., & Goto, T. 2005, *AJ*, 130, 1535
 Grebel, E. K., Gallagher, J. S., & Harbeck, D. 2003, *AJ*, 125, 1926
 Gunn, J. E., & Stryker, L. L. 1983, *ApJS*, 52, 121
 Guzmán, R., Gallego, J., Koo, D. C., Phillips, A. C., Lowenthal, J. D., Faber, S. M., Illingworth, G. D., & Vogt, N. P. 1997, *ApJ*, 489, 559
 Hammer, F., Gruel, N., Thuan, T. X., Flores, H., & Infante, L. 2001, *ApJ*, 550, 570
 Homeier, N. L., et al. 2005, *ApJ*, 621, 651
 King, I. R. 1972, *ApJ*, 174, L123
 Kobulnicky, H. A., & Zaritsky, D. 1999, *ApJ*, 511, 118
 Kodama, T., Smail, I., Nakata, F., Okamura, S., & Bower, R. G. 2001, *ApJ*, 562, L9
 Koo, D. C., Bershad, M. A., Wirth, G. D., Stanford, S. A., & Majewski, S. R. 1994, *ApJ*, 427, L9
 Koo, D. C., Guzman, R., Gallego, J., & Wirth, G. D. 1997, *ApJ*, 478, L49
 Kron, R. G. 1995, in *The Deep Universe*, ed. B. Bingeli & R. Buser (New York: Springer), 233
 Landolt, A. U. 1992, *AJ*, 104, 340
 Lotz, J. M., Martin, C. L., & Ferguson, H. C. 2003, *ApJ*, 596, 143
 Lubin, L. M., Mulchaey, J. S., & Postman, M. 2004, *ApJ*, 601, L9
 Martin, C. L., Lotz, J., & Ferguson, H. C. 2000, *ApJ*, 543, 97
 Massey, P., Strobel, K., Barnes, J. V., & Anderson, E. 1988, *ApJ*, 328, 315
 Oemler, A. J., Dressler, A., & Butcher, H. R. 1997, *ApJ*, 474, 561
 Phillips, A. C., Guzman, R., Gallego, J., Koo, D. C., Lowenthal, J. D., Vogt, N. P., Faber, S. M., & Illingworth, G. D. 1997, *ApJ*, 489, 543 (P97)
 Poggianti, B. M., et al. 2001, *ApJ*, 562, 689
 Postman, M., Lubin, L. M., & Oke, J. B. 2001, *AJ*, 122, 1125
 Rakos, K. D., & Schombert, J. M. 1995, *ApJ*, 439, 47
 Tran, K. H., van Dokkum, P., Illingworth, G. D., Kelson, D., Gonzalez, A., & Franx, M. 2005, *ApJ*, 619, 134
 Werk, J. K., Jangren, A., & Salzer, J. J. 2004, *ApJ*, 617, 1004